• Volume 7C, Number 4, December 1959

מוסד ויצמן למדעים במדעי הטבע ובטכנולוגיה בישראל • ירושלים • The Weizmann Science Press of Israel • Jerusalem

BULLETIN OF THE RESEARCH COUNCIL OF ISRAEL

Section C TECHNOLOGY

Bull. Res. Counc. of Israel. C. Techn.

Incorporating the Scientific Publications of the Technion — Israel Institute of Technology, Haifa

• Volume 7C, Number 4, December 1959

מוסד ויצמן למדעים במדעי הטבע ובטכנולוגיה בישראל • ירושלים
The Weizmann Science Press of Israel • Jerusalem

BULLETIN OF THE RESEARCH COUNCIL OF ISRAEL

Section C TECHNOLOGY

Bull. Res. Counc. of Israel. C. Techn.

Incorporating the Scientific Publications of the Technion — Israel Institute of Technology, Haifa

BULLETIN
OF THE RESEARCH COUNCIL
OF ISRAEL

MIRIAM BALABAN
Editor

NOTICE TO CONTRIBUTORS

Contributors to the *Bulletin of the Research Council of Israel* should conform to the following recommendations of the editors of this journal in preparing manuscripts for the press.

Contributions must be original and should not have been published previously. When a paper has been accepted for publication, the author(s) may not publish it elsewhere unless permission is received from the Editor of this journal.

Papers may be submitted in English and in French.

MANUSCRIPT

General

Papers should be written as concisely as possible. MSS should be typewritten on one side only and double-spaced, with side margins not less than 2.5 cm wide. Pages, including those containing illustrations, references or tables, should be numbered.

The Editor reserves the right to return a MS to the author for retyping or any alterations. Authors should retain copies of their MS.

Spelling

Spelling should be based on the Oxford Dictionary and should be consistent throughout the paper. Geographic and proper names in particular should be checked for approved forms of spelling or transliteration.

Indications

Greek letters should be indicated in a legend preceding the MS, as well as by a pencil note in the margin on first appearance in the text.

When there is any room for confusion of symbols, they should be carefully differentiated, e.g. the letter "l" and the figure "1"; "O" and "0".

Abbreviations

Titles of journals should be abbreviated according to the *World List of Scientific Periodicals.*

Abstract

Every paper must be accompanied by a brief but comprehensive abstract. Although the length of the abstract is left to the discretion of the author, 3% of the total length of the paper is suggested.

References

In Sections A and C, and in Letters to the Editor in all Sections, references are to be cited in the text by number, e.g. ... Taylor[3] ..., and are to be arranged in the order of appearance.

In Sections B, D, E, and G, the references are to be cited in the text by the author's name and date of publication in parentheses, e.g. .... (Taylor 1932)... If the author's name is already mentioned in the text, then the year only appears in the parenthesis, e.g. ... found by Taylor (1932).... The references in these Sections are to be arranged in alphabetical order.

In Section F, references are to be cited in the text by number in square brackets, e.g. ... Taylor[3] .., and are to be arranged in alphabetical order.

The following form should be used:

3. TAYLOR, G. I., 1932, *Proc. roy. Soc.*, **A138**, 41.

Book references should be prepared according to the following form:

4. JACKSON, F., 1930, *Thermodynamics*, 4th ed., Wiley, New York.

TYPOGRAPHY

In all matters of typography the form adopted in this issue should be followed. Particular attention should be given to position (of symbols, headings, etc.) and type specification.

ILLUSTRATIONS

Illustrations should be sent in a state suitable for direct photographic reproduction. Line drawings should be drawn in large scale with India ink on white drawing paper, bristol board, tracing paper, blue linen, or blue-lined graph paper. If the lettering cannot be drawn neatly by the author, he should indicate it in pencil for the guidance of the draftsman. Possible photographic reduction should be carefully considered when lettering and in other details.

Half-tone photographs should be on glossy contrast paper.

Illustrations should be mounted on separate sheets of paper on which the caption and figure number is typed. Each drawing and photograph should be identified on the back with the author's name and figure number.

The place in which the figure is to appear should be indicated in the margin of the MS.

PROOFS

Authors making revisions in proofs will be required to bear the costs thereof. Proofs should be returned to the Editor within 24 hours, otherwise no responsibility is assumed for the corrections of the author.

REPRINTS

Reprints may be ordered at the time the proof is returned. A table designating the cost of reprints may be obtained on request.

Orders in America should be addressed to Interscience Publishers Inc., New York, N. Y., and in England and Europe to Wm. Dawson and Sons, Ltd., Cannon House, Macklin Street, London, W. C 2, directly or through booksellers. — Annual subscription per section (four issues): IL. 6.000 ($6.00, £2.20). Single copy: IL. 1.500 ($1.50, 12s.) — Manuscripts should be addressed: The Editor, The Weizmann Science Press of Israel, P.O.B. 801, Jerusalem, 33 King George Ave. Telephone 62844

AN INVESTIGATION OF THE MARTENSITIC AREA OF THE TIME-TEMPERATURE TRANSFORMATION DIAGRAM OF A HIGH-SILICON CARBON STEEL

A. Rosen and A. Taub

Israel Institute of Metals, Technion–Israel Institute of Technology, Haifa

ABSTRACT

The quenching characteristics of a silicon steel were investigated. The main object of the study was the determination of the initial point of the martensitic transformation (M_S line in time-temperature transformation diagram) as well as the percentage transformation at different temperatures, with a view to obtaining a diagram showing the degree of transformation as a function of temperature. The equation approximating the experimental curve was also found.

High-silicon steel of the composition: C—0.67%, Mn—0.61%, Si—1.85%, P—0.025%, S—0.01%, Cr—0.11% is finding more and more use in the manufacture of springs and tools, and the exact determination of its characteristics is accordingly of growing importance. The main object of the present study was the determination of the initial point of the martensitic transformation (M_S) as well as the percentage transformation at different temperatures, using the microscopic technique developed by Greninger and Troiano[1].

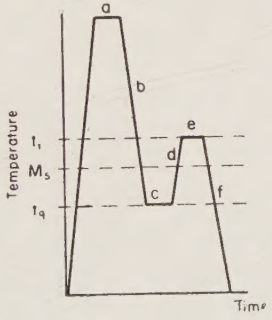

Figure 1
Schematic description of heat treatment

The procedure is described schematically in Figure 1. A small specimen is austenitised (step a) and subsequently transferred (step b) to a quenching bath of liquid metal at temperature t_q (below the estimated M_S point) at which it is kept long enough to ensure a uniform temperature distribution (step c). This results in the formation of a certain amount of martensite in equilibrium with retained austenite

Received April 15, 1959

Figure 2
Magnification × 2000 Etch: nital 4%
Specimen quenched in 220°C liquid metal bath
Light-etch martensite — 89%; dark-etch martensite — 11%

Figure 3
Magnification × 2000 Etch: nital 4%
Specimen quenched in 160°C liquid metal bath
Light-etch martensite — 36.3%; dark-etch martensite — 63.7%

at the given temperature. The specimen is then transferred very rapidly (step d) to a tempering bath and kept in it as above at temperature t_t (step e). This in turn results in tempering of the martensite, while the austenitic fraction remains unchanged. As a final step (f), the specimen is transferred to a water quenching bath at room temperature, where the remaining austenite is transformed into martensite. The specimen thus contains both tempered and fresh martensite, differentiated under the microscope through the selective action of the etching medium (nital), which reveals them as dark- and light-etch areas respectively. The lowest temperature to yield only light-etch martensite in the microstructure represents the required M_S point, and the highest to yield only dark-etch martensite, the M_f point.

In the present experiments, specimens 8 mm in diameter and 2 mm thick were treated, in three parallel series, at successive quenching temperatures from 250°C down to room temperature in 10°C intervals. Two low-melting metal baths were used, one maintained at a constant temperature of 300°C (t_t) and the other varied according to the quenching temperature required. Each specimen was placed in the heating chamber of the furnace for five minutes at the austenitising temperature (830°C) and then successively transferred to the quenching bath for ten seconds, to the tempering bath for seven seconds, and finally to the water bath. As it was found that no further changes take place at quenching temperatures below 100°C, the latter was accepted as the lower limit of measurement, except for one additional test at 0°C as control. The treated specimens were subjected to microscopic examination, in which the relative proportions of light and dark areas in the microstructure (as shown in Figures 2 and 3) were determined by Rosiwal's method of linear analysis[2], based on measuring line intercepts across the different areas in a number of random directions (three in the present case, making a total of nine measurments per series)*.

The mean, standard deviation, and standard error of the mean were calculated from the readings obtained for each series. The average for each quenching temperature was plotted in the diagram shown in Figure 4, giving the martensite content (in percent) as a function of temperature. It was found that the points could only be joined by a cubic curve, for which the following polynomial approximation was obtained:

$$M = 95 - 0.0236(t - 100) - 0.00962(t - 100)^2 + 0.0000322(t - 100)^3.$$

(temperature in Centigrade)

It was established that the martensitic transformation sets in at 230°C and ends for all pratical purposes, as already mentioned, at 100°C. The amount of residual austenite at room temperature was approximately 4%. It was also established that although the M_S point varies with the composition[3], grain size[4] (in the present case—ASTM Standard No. 3) and austenitising conditions[5], the character of the curve is the same irrespective of the treatment. This is evident from the fairly close agreement

* In order to eliminate the operative error factor, the specimens were tested completely at random instead of in the order of treatment.

with the results obtained by Cohen[3], who found that the amount of martensite formed at a given temperature is primarily a function of the difference $M_S - t_q$,

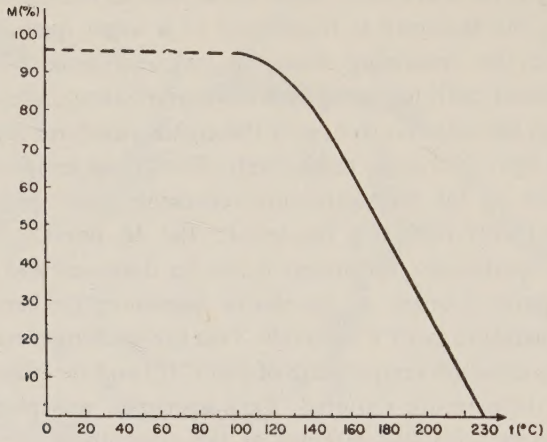

Figure 4

Martensite content vs. quenching temperature
(dashed line represents the 0—100°C interval, below the lower limit of measurement).

irrespective of composition, grain size and austenitising conditions, and proposed the following empirical formula[5]

$$M = 100 \times 3.05 \times 10^{-14} \times [820 - (M_S - t_q)]^{5.32}$$

(temperatures in degrees Fahrenheit)

The formula was derived for steels containing 0.75–1.35%C, up to 2.8%Cr and 5.4%Ni, and the agreement with the entirely different high-silicon steel used in the present experiments is seen from the following table:

Quenching temperature (°C)		220	200	180	160	140
Martensite content	Cohen's formula	14	32.5	48	60	70
	Present experiments	10	28	48	65.5	80

REFERENCES

1. GRENINGER, A. B. and TROIANO, A. R., Kinetics of the Austenite–Martensite Transformation in Steel, *Trans. ASM*, **28**, 537.
2. ROSIWAL, A., 1898, Über geometrische Gesteinsanalysen. Ein einfacher Weg zur ziffermaessigen Feststellung der Mineralbestandteile gemengter Gesteine, *Verhandlungen der K.K. Geologischen Reichsanstalt*, **5-6**, 143.
3. COHEN, M., 1948, *The Martensite Transformation*, presented at Conference on Phase Transformation in Solids, National Research Committee on Solids, Cornell University.
4. BARNETT, W. I. and TROIANO, A. R., 1948, The Effect of Grain Size on the Martensitic Transformation, *AIME Technical Note No.* 4.
5. COHEN, M., 1948, Retained Austenite, Edward De Mille Campbell Memorial Lecture, *Trans. ASM*, **41**, 35.

STRAIN DISTRIBUTION IN THE MICROSTRUCTURE OF PLASTICALLY DEFORMED STEEL

D. BEN-ISRAEL AND A. TAUB

Israel Institute of Metals, Technion–Israel Institute of Technology, Haifa

ABSTRACT

The inhomogeneous distribution of tensile strain in the microstructure of polycrystalline ferritic steel specimens was studied by means of micro-hardness tests. The grain boundary region showed higher hardness compared with the grain interior, with the minimum difference at 4% elongation.

Extensive studies have been carried out on the inhomogeneous nature of plastic deformation in metals, mainly aluminium. In their study of coarse-grained aluminium in tension, Carpenter and Elam[1] found the least amount of strain near the grain boundaries, while Aston[2] arrived at a similar conclusion by observing changes in intragranular orientation. Hanson and Wheeler[3] tested polished specimens at 250°C and showed that at slow rates of strain the grain boundaries underwent heavy deformation, while at rapid rates first deformation took place in the interior. Barrett and Levenson[4] showed that the intragranular deformation in a polycrystalline specimen is governed by the orientation of the surrounding grains.

In the present study steel specimens were used, in which different amounts of strain were produced by tensile loading in the plastic range. Determination of the intragranular strain distribution by direct measurement being practically impossible, an indirect method based on micro-hardness tests was adopted.

The commercial grade low-carbon steel selected for the experiments had the following composition: C = 0.07%, Mn = 0.39%, P = 0.037%, S = 0.03%, and its original grain size was A.S.T.M. No. 7. The steel was subjected to a coarsening treatment by means of successive straining and recrystallisation (average grain diameter of 0.6 mm). The specimens were metallographically polished and strained to elongations of 2, 4, 8, 12, 16 and 20 percent on a Hounsfield tensometer (gauge length 10 mm, limit of accuracy ± 0.005 mm; six specimens in each series). After subsequent repolishing, for the elimination of surface roughness introduced during straining, specimens were subjected to macro- and micro-hardness measurements, using

Received May 15, 1959.

the Vickers diamond-pyramid method (100 g load)*, with ten random indentations made in each specimen, indentation diagonals measured at ×250 magnification, and a band of 0.1 mm width assumed as the boundary region. The averages calculated for each elongation are given in Table I and Figure 1.

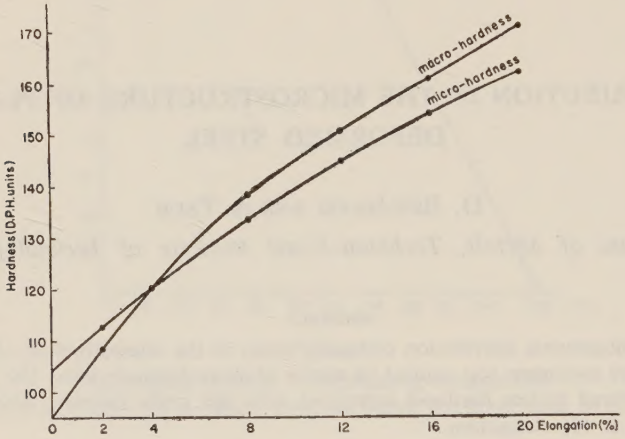

Figure 1
Average macro- and micro-hardness values vs. elongation

The diagrams in Figure 2 give the frequency distribution of the hardness values over the whole of the specimen (calculated for value groups in 5 D.P.H. intervals), and show that the distribution range increases with the elongation. The diagrams in Figures 3 and 4 give the frequency distribution of the hardness values for grain interiors and boundaries respectively. In all diagrams, common curves were drawn through the average points.

The main finding (as can be seen from the table) was that, of 100 grains examined, 95 had a boundary hardness higher than that of the interior, with the minimum difference for the 4% elongation. The physical significance of this finding will be the subject of further study.

---

* The 100 g load was adopted because of the following considerations:

1) Loads under 70 g rendered the test over-sensitive; in spite of the fact that the specimens consisted of very low-carbon steel with homogeneous distribution of large coagulated carbide particles — whose immediate neighbourhood was carefully avoided — abrupt jumps were observed in hardness measurements, probably due to phenomena outside the scope of the present study.

2) Loads over 150 g, on the other hand, rendered the test insufficiently sensitive owing to the large area of indentation — under these circumstances, hardness variations due to intragranular strain could not be detected.

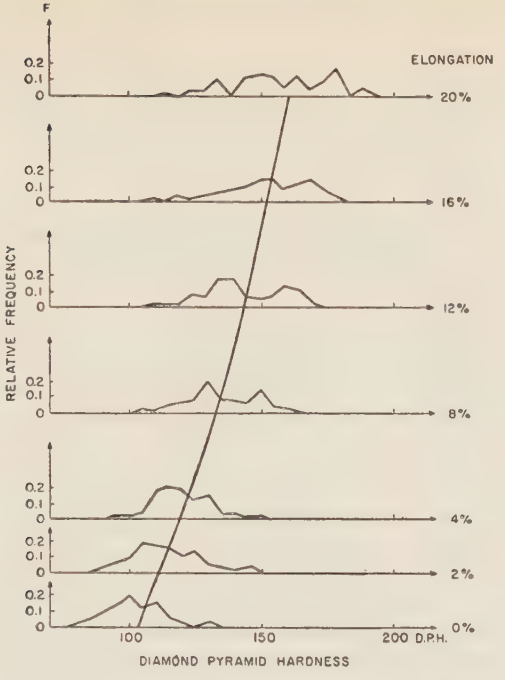

Figure 2
Relative frequency polygons of micro-hardness values over the whole of the specimen

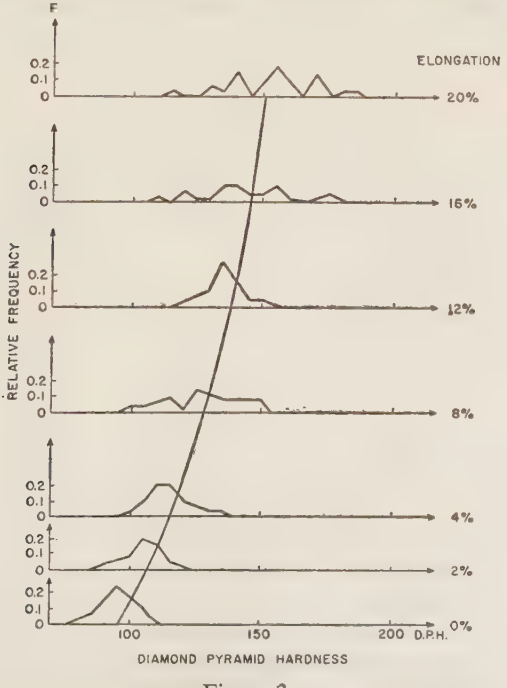

Figure 3
Relative frequency polygons of micro-hardness values for grain interiors

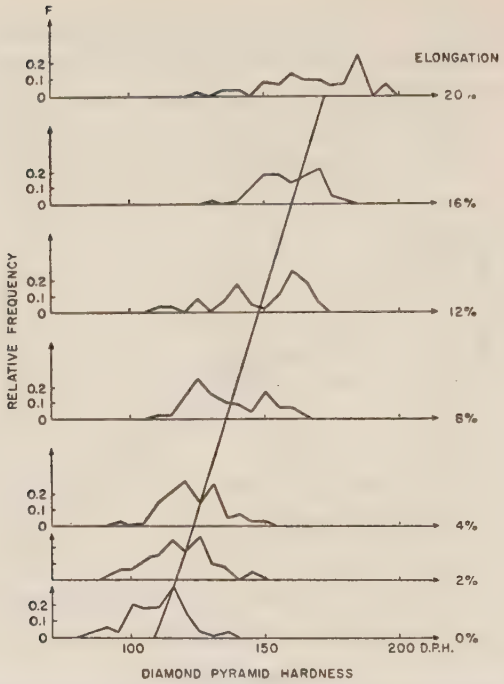

Figure 4
Relative frequency polygons of micro-hardness values for grain boundaries

TABLE I
Average hardness values vs. elongation

Elongation (%)	Corresponding (Rockwell A) Macro-hardness converted into D.P.H. units	Micro-hardness	Interior hardness	Boundary hardness
		(D.P.H. units)		
0	95	104	96	109
2	108	112	106	116
4	120	120	115	123
8	138	132	127	135
12	150	144	137	150
16	160	153	145	160
20	170	161	152	170

REFERENCES

1. Carpenter, H. C. H. and Elam, C. F., 1921, *Proc. Roy. Soc.*, **A100**, 329.
2. Aston, R. K., 1927, *Proc. Camb. Phil. Soc.*, **23**, 549.
3. Hanson, D. and Wheeler, M. A., 1931, *Journal Inst. of Met.*, **62**, 307.
4. Barrett, C. S. and Levenson, L. H., 1940, *Trans. A.I.M.M.E.*, **137**, 112.

PLASTIC HINGE MODELS

A. Zaslavsky

Technion–Israel Institute of Technology, Haifa

In Limit Design, mild steel is usually assumed to be an "ideal plastic material" (the so-called St. Venant body)[1,2].

Another concept used is the "plastic hinge", denoting a beam section subjected to the "full plastic moment" M_{pl}. This state is reached (Figure 1) when stress distribution approaches two rectangles (no buckling assumed); the small inclination of the segment n–n at the neutral axis is neglected. Plane sections are assumed to remain plane also in the plastic stage.

The plastic hinge behaves like an ordinary hinge after M_{pl} has developed, provided the rotation is in the same sense as M_{pl}. If the rotation is reversed, the response of the section is elastic. In Figure 2 the resistance moment M is plotted against the strain ε of the extreme fibre (ε is proportional to the curvature $\Delta\varphi$); M_{YP} denotes the maximum

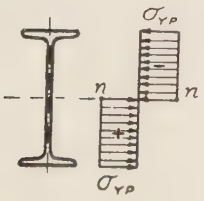

Figure 1

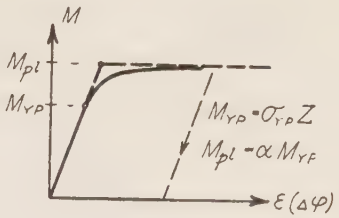

Figure 2

elastic moment. The curved segment between M_{YP} and the asymptotic M_{pl} represents the elastic–plastic stage (the section has an elastic core) and its shape depends upon the 'shape factor' α of the section (for a rectangle $\alpha = 1.5$, for a rolled I section $\alpha \cong 1.16$). Further idealisation may be obtained by replacing the curved segment by extending the elastic range up to M_{pl} (dashed lines in Figure 2). Thus an idealised trapezoidal diagram is obtained (analogous to the σ/ε diagram) which would be quite accurate in the case of an I section with a very thin web and thin flanges ($\alpha \to 1.0$).

Received April 15, 1959

Figure 3 shows the suggested model for the ideal plastic section, representing a combination of two St. Venant-body models. A rotational type of model would consist of two rings A and B with constant friction between them, the inner ring connected to a fixed axis C by means of a spiral spring D (Figure 4).

In limit design of frames and beams, all plastic deformations are assumed to be concentrated at the plastic hinges and elastic deformations between the hinges are neglected. Each formation of a plastic hinge reduces the statical indeterminacy of the structure by one. The critical (collapse load) stage is reached when a sufficient number of hinges has formed to transform the structure (or part of it) into a mechanism. Thus, the behaviour of the structure will be better understood if the plastic hinge model is imagined as incorporated into the beam. It is suggested that in this case the plastic hinge may be conveniently represented by a bolted connection (Figure 5a), the nut being tightened so as to produce friction equivalent to M_{pl} of the beam section[3]. The absolute rigidity of this model in the elastic stage (Figure 5b) does

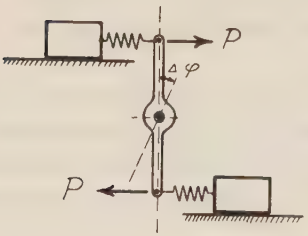

Figure 3

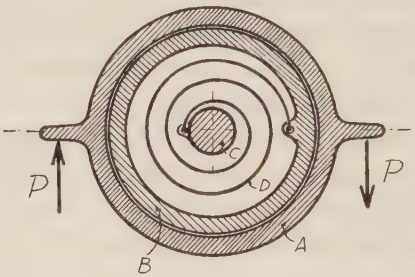

Figure 4

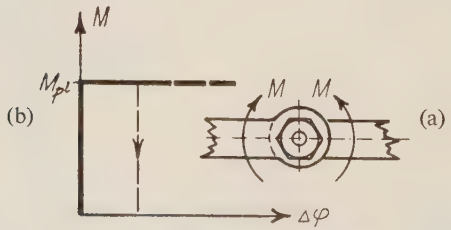

Figure 5

not affect the general behaviour of the structure. Figure 6 shows, for example, the collapse mechanism of a two-span beam of constant section under a force P at the left span. The critical (collapse) load P_{cr} may be readily found using the virtual work

method (φ denotes the virtual rotation at the hinges): $P_{cr} \times 1.0 = M_{pl} \times 2\varphi + M_{pl}\varphi = 3M_{pl}\varphi = 6M_{pl}/l$. The same result may be read from the moment diagram.

By comparison, the maximum elastic load equals in this example $P_{YP} = \frac{64}{13} M_{YP}/l \cong 4.9\ M_{YP}/l$. Assuming an I-beam with $\alpha = 1.16$ we have ($M_{pl} = \alpha M_{YP}$): $P_{cr} \cong 7\ M_{YP}/l = 1.43\ P_{YP}$.

In the case of distributed loads the position of the plastic hinge (M_{max}) can, as usual, be determined from the equation

$$\partial M/\partial x = 0.$$

This equation is based on the equilibrium condition only, which also holds in the full plastic stage just prior to the formation of the collapse mechanism.

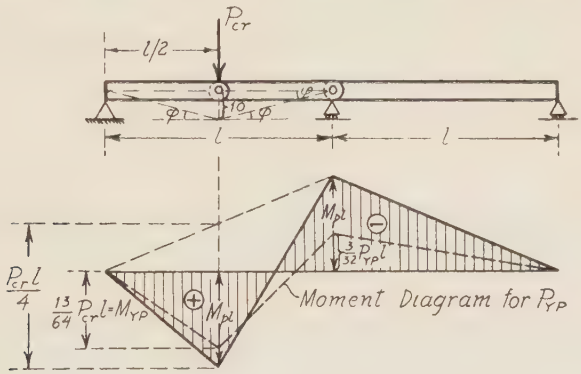

Figure 6

During the elastic-plastic stage the M_{max} point keeps shifting owing to the redistribution of the bending moment diagram.

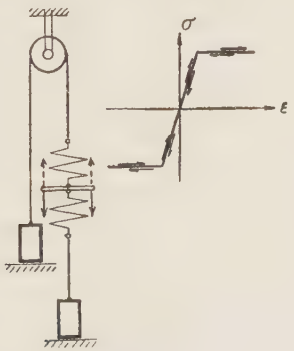

Figure 7

It may be noted that the model of Figure 7 would represent a hypothetical material where no energy is dissipated; the model works in both directions.

REFERENCES

1. Reiner, M., 1949, *Twelve Lectures on Theoretical Rheology*, North-Holland Publishing Co., Amsterdam.

2. Zaslavsky, A., 1955, *Ultimate Load Design of Steel and Reinforced Concrete Structures*, Haifa (in Hebrew).

3. Zaslavsky, A., 1954, Mechanics of Materials, *Engineering Handbook* (S. Ettingen, editor), Vol. I, Tel-Aviv (in Hebrew).

A PRELIMINARY NOTE ON THE USE OF CATION EXCHANGE CAPACITY OF CITRUS JUICES AS A RAPID SCREENING TEST FOR THE DETECTION OF ADULTERATIONS

Y. Pomeranz, J. J. Monselise and C. Lindner

Food Testing Laboratory, Ministry of Trade and Industry, Haifa, and Laboratory of Assis Ltd., Ramat Gan

ABSTRACT

A screening test is proposed for the detection of adulterations of citrus juices, based on the cation exchange capacity of the juices. Details of the method and results are reported.

Several tests have been recommended in order to detect adulterations of citrus juices. These tests are generally carried out in addition to the usual T.S.S., acidity and ascorbic acid determinations to check some less known constants which are more difficult to bring into their correct ranges when trying to adulterate juices.

For many years the formol titration[1] and chloramine value[2] have been accepted as criteria of the genuineness of citrus juices. Other tests have been suggested[3] and discussed[4,5,6]. Safina and Trifirò[7] suggested a modification of the chloramine value method of Tillmans and Hollatz. Some values for formol titrations and chloramine values of citrus juices have been reported[5,6,7]. Benk suggested the use of the ratio: total acid/formol titration; this value must be between 1:11.5 and 1:22.4 for orange juice and between 1:2.3 and 1:4.1 for lemon juice. He suggested that formol values between 1.4 and 2.6 be accepted for genuine orange juice. Safina and Trifirò report chloramine values between 11.14 and 17.97 for orange juice and between 9.20 and 14.52 for lemon juice. They point out the disturbing influence of the essential oils on the chloramine value, and they suggest the use of petrol ether extraction before the chloramine titration is carried out. Benk[8] published additional work on the determination of the juice content in fruit drinks by chloramine T.

Ash determination and ash composition (P, K, Ca, alkalinity) have been widely used for the same purpose for many years and are generally accepted as the most reliable criteria.

The formol and chloramine titrations suffer from the drawback of too wide

Received July 14, 1959

fluctuations of their values and the ash and connected determinations are too time-consuming to be used as a rapid screening tool.

We tried to use the cation exchange capacity of the citrus juices as a quick screening test to establish their genuinity. The fluctuations of the values obtained by this method are reasonably limited and it can efficiently be used as a very rapid substitute for ash determinations.

The method simply determines the difference between a direct acidimetric titration of the juice and the titration carried out after exchanging the cations present in the juice with H^+. This Δ of course is proportional to the amount of salts, and can be used as a counterpart of the T.S.S., acidity, ascorbic acid titrations, and as an additional and more accurate screening tool to confirm and complete the conclusions reached by formol and chloramine titrations.

EXPERIMENTAL

Materials

Jaffa orange juice, fresh and canned with and without addition of sucrose.

In addition, adulterated juices, whose compositions are reported later. Duolite C 20 cation exchange resin (capacity 4 milliequivalents per ml).

Preparation of the cation exchange column

A 14 mm × 300 mm column of Duolite C 20 was packed in a 100 ml glass buret fitted with a tap. Glass wool pads were placed on the top and bottom of the column. The resin was regenerated with 100 ml of 10% HCl and washed with water until 50 ml of the effluent required less than 0.05 ml of 0.1N NaOH for neutralization using phenolphtalein as an indicator. The regenerating solution was passed through the column at a rate of 8–10 ml per minute.

Analytical procedure

100 ml of juice were partially clarified by centrifugation (1400 r.p.m.; 3–4 min.). The supernatant liquid was filtered through a cottonwool pad. 10 ml of the filtrate were titrated with 0.1N NaOH (phenolphthalein indicator). Let A be the volume of NaOH used (in mls.).

50 ml of the filtrate were passed through the resin column at a rate of 6–8 ml per min. The column was subsequently washed with 150 ml of water. From the total volume of the effluent (200 ml) 50 ml were titrated with 0.1N NaOH. Let B be the volume (in mls.) of NaOH used in this titration.

Let $\Delta = (B \times 8 - A \times 10) : 10 =$ ml N NaOH, corresponding to the cation exchange capacity of the juice. The ash was determined on 10 ml of centrifuged and filtered

juice, by evaporating it in a porcelain basin and by incinerating the residue in a thermostatically controlled muffle-oven at 600°C. The T.S.S. were determined refractometrically.

RESULTS

The results are reported in the following table. Samples marked (*) contained added sugar. All other samples were straight Jaffa orange juices. A was diluted with 30% water. B was prepared by blending 80% juice, 10% orange cells, 10% water. D contained 30% orange peel (disintegrated) and 70% water. A, B, C, D, were standardized at 12.0 T.S.S. by addition of sucrose. B may be labelled as a "pulpy juice". C is on the borderline of the adulteration. D is a gross falsification.

TABLE I

Sample No.	Ash (g/100 ml juice)	Δ (ml N NaOH/100 ml juice)	Ash/Δ factor	T.S.S.
1	0.311	4.8	0.065	—
2	0.293	4.9	0.060	—
3	0.308	5.1	0.061	13.5*
4	0.329	4.5	0.074	14.0*
5	0.310	5.0	0.062	12.4
6	0.301	4.8	0.064	14.0*
7	0.306	4.9	0.063	12.5*
8	0.313	4.9	0.064	11.8
9	0.329	5.2	0.063	11.8
10	0.323	5.3	0.061	11.6
11	0.331	5.2	0.064	—
12	0.307	4.9	0.063	—
13	0.337	5.0	0.067	11.8
14	0.344	5.2	0.066	12.5
15	0.275	5.2	0.054	—
16	0.258	4.8	0.054	12.4
17	0.296	5.3	0.058	—
18	0.279	4.7	0.059	10.6
A	0.220	3.8	0.058	12.0
B	0.302	4.8	0.064	12.0
C	0.294	4.5	0.066	12.0
D	0.072	1.6	0.045	12.0

CONCLUSIONS

From the above results it is possible to establish a Δ of 4.5 as the lower admissible limit for a genuine Jaffa orange juice. This value is suggested as a criterium for screening purposes only, but we consider that it is a workable figure, because the values of the ash/Δ factor are reasonably consistent.

More work must be carried out on different varieties of oranges as well as on lemon and grapefruit.

REFERENCES

1. Tillmans, J. and Kiesgen, 1927, *Zeitschr. Untersuchung Lebensm.*, **53**, 132.
2. Tillmans, J. and Hollatz, G., 1929, *ibid.*, **57**, 489.
3. Solarino, E., 1946, *Citrus*, **18**, 12.
4. Buffa, A., 1954, *Industria Conserve*, **29**, 118.
5. Benk, E., 1956, *Fruchtindustrie*, **1**, 226–231.
6. Benk, E., 1956, *ibid.*, **1**, 118–121.
7. Safina e Trifiro, 1957 (March), *Conserve e derivati Agrumari*, **21**.
8. Benk, E., 1958, *Naturbrunnen*, **8**, 185–6.

CERAMIC AND CERMET FUEL ELEMENTS IN POWER REACTORS

(Literature Survey)

J. Barta

Department of Refractories Technology, University of Sheffield

ABSTRACT

To design power reactors economically higher fuel temperatures and burn-ups must be achieved. The uranium metal fuel element (pure or alloyed) cannot be used at temperatures higher than 600°C and burn-ups higher than 5000 MWD/T, because of severe radiation damage causing dimensional instability of the fuel element.

The oxides, carbides, nitrides and silicides of uranium are refractory compounds and have suitable properties to make them useful as high temperature fuel elements. Good resistance to radiation damage and fission products retention up to 1500°C and 10,000 MWD/T burn-up have been observed for uranium dioxide (thermal conductivity being poor, however). Uranium carbide has better thermal properties and should behave as well under irradiation as uranium dioxide; the nitrides and silicides, while promising in certain respects, have not been sufficiently investigated.

By dispersing the ceramic particle in a metallic matrix, thus obtaining a cermet, improvement in mechanical and thermal properties can be achieved. However, the parasitic neutron absorption of such a fuel element may be high, depending on the matrix metal, and enriched uranium must eventually be used.

While the use of ceramic and cermet fuel elements removes limitations of fuel temperature and burn-up, it raises special problems to which solutions must be found.

NOMENCLATURE

Burn-up — depletion of fissionable material during reactor operation.
Cladding — metal covering of fuel element to protect it against corrosion and retain fission products.
Coolant — fluid pumped through reactor in order to remove energy released in fission in form of heat and transfer heat to power generating equipment.
Critical — capable of sustaining a chain reaction at a constant level.
Cross section (microscopic, neutron) (σ) — effective area per nucleus for a nuclear reaction, expressed in barns ($=10^{-24}$ cm^2).
Fertile material — material capable of conversion into fissile material through a nuclear transformation.
Fissile material — nuclear reactor material subject to fission.
MWD/T — megawatt-day per ton uranium.

INTRODUCTION

The experience of the last five years has shown that the use of atomic energy for generating power on an industrial scale is feasible. The next step in this development is more economical design of atomic power plants, so as to put them on a competitive basis.

Received November 25, 1959

Two improvements are essential to this goal:

1. Higher fuel temperatures, for higher efficiency in the conversion of heat into electric energy (as, for instance, in a closed-cycle gas turbine system with thermal efficiencies up to 40%).

2. Running the fuel elements to higher burn-ups so as to lengthen their life and obtain more kWh per unit uranium.

Most power reactors in use or under construction are based on the natural uranium fuel cycle U^{235}–U^{238} which seems the most economical under present circumstances; there are sufficient reserves of fissionable U^{235} to sustain a nuclear power economy for perhaps the next hundred years. Other possible fuel cycles are Pu^{239}–U^{238} and U^{233}–Th^{232}. Both necessitate processing highly radioactive materials (Pu^{239} and U^{233}), which accordingly affects fabrication costs. It is not expected that thorium and plutonium burning systems should play an important part in the development of power reactors before 1970.[1]

The following discussion will therefore be limited mainly to uranium.

A universal effort is being made to increase the working temperatures of the fuel elements.

The Calder Hall reactors work to a maximum uranium temperature of 480°C, with an average fuel life of one year and a burn-up of 1500 MWD/T. The new Hunterston reactor[2], also fuelled with metallic uranium, will have a maximum fuel temperature of 570°C, an average fuel life of 5 years and a burn-up of 4500 MWD/T. The Italian Latina reactor, scheduled to go critical in 1962, will also operate with natural uranium rods at a maximum temperature of 585°C. (The coolant is CO_2, with an outlet temperature of 390°C and inlet temperature of 180°C).[3] These are about the maximum temperatures and burn-ups at which reactors based on pure or alloyed uranium can operate. To reach gas coolant outlet temperatures of 550°C and later of 750°C, with fuel temperatures higher than 1000°C and burn-ups of 10,000–15,000 MWD/T, the uranium metal will have to be replaced by ceramics or cermets. Only this will enable the atomic power plant to compete with advanced coal or oil burning plants.[4, 5]

It is imperative that Israel, which is to face in the next few years the necessity of a significant energy production[6] and which to-day is heavily dependent on imported conventional fuel, follow closely these developments and problems.

THE LIMITATIONS OF URANIUM METAL AS FUEL

While the melting point of uranium is 1132°C, the working temperature limit of uranium fuel elements is much lower. Uranium undergoes two phase changes:

$$\text{Alpha-uranium (orthorhombic)} \xrightarrow{660^\circ C} \text{beta-uranium(tetragonal)} \xrightarrow{774^\circ C} \text{gama-uranium (body-centred cubic).}$$

These changes are accompanied by corresponding volume changes, and thermal cycling through the alpha → beta transformation point causes a rapid change in the shape of uranium specimens and leads to porosity; the drop in density after 1,000 cycles is 30%. The alpha and beta phases are anisotropic and thermal cycling within the alpha range may cause an increase in length of several 100% and severe surface wrinkling[7,8,9]. The uranium fuel element is also subjected to very severe radiation, the most important factors being the neutrons and fission products. While several effects of this radiation on the properties of the metal are significant, the most damaging are swelling, due to gaseous fission products (xenon and krypton) and an increase in the creep rate under irradiation and at high temperatures. A volume of 4.4 cm^3 of gases at S.T.P. per cm^3 metal is produced for each percent of atoms fissioned, and as the temperature is higher the pressure exerted increases while at the same time the creep strength of the metal is reduced. As a result[10], a 10–40% increase in volume is observed in the range of 500°–800°C. Since this volume change cannot be accommodated, it leads to blocking of the coolant channels, cladding failure, damage and distortion of the heat transfer surfaces, and discharge difficulties.

A great deal has been done to improve the properties of uranium metal either by thermal treatment[11] or by alloying[11,12,13] but no improvement permits fuel working temperatures above 600°C and burn-ups higher than 5,000 MWD/T. Even so, volume changes of several percent are observed and must be allowed for by the designer. Another undesirable feature of uranium metal is its very poor corrosion resistance to most coolants; any failure of the cladding would result in a highly undesirable contamination of the system.

CERAMIC FUEL ELEMENTS

The oxides, carbides, nitrides and silicides of fertile and fissile elements are included in this group. These materials are solids mainly ionic in character, and their properties are different from those of the metals. The requirements of high temperature fuel elements which should be satisfied by ceramics may be summarised as follows:

a) High melting point, and absence of phase changes up to the melting point.
b) Low thermal neutron absorption cross section (for thermal reactors).
c) Resistance to irradiation at high temperatures.
d) Retention of fission products at high temperatures.
e) Resistance to corrosion at high temperatures.
f) Thermal conductivity and thermal shock resistance.
g) Sufficient mechanical strength at high temperatures.
h) Low fabrication cost.

It is fortunate that a number of uranium compounds have very high melting points and good structural stability. The properties of these compounds are described in Table I.

It must be realised that using a uranium compound as atomic fuel means dilution of the pure uranium and, therefore, a waste of neutrons. For a natural uranium

TABLE I

Ceramic compounds of fissile or fertile elements

Compound	m.p. (°C)	Uranium density (g/cm^3)	Thermal conductivity at °C (kcal/cm.sec.)	Corrosion resistance*	Mechanical strength
U	1132	19.0	200°C–0.07 500°C–0.08	Oxidised by air and water at l.t. Reacts with CO_2 at 500°C. Reacts with N_2,H_2	Ult. tensile strength 100,000 lb./sq.in.
UO_2	2880	10.5	800°C–0.007 1,000°C–0.005 1,400°C–0.003	Resistant to water (300°C), CO_2 (900°C), Na, K, He, H_2. Oxidised by air at h.t.	Bending strength 16,000 lb/sq.in. (1000°C)
UC	2350	13.0	260°C–0.05 700°C–0.06	Reacts with H_2O and air at l.t. Resistant to CO_2 (up to 500°C), Na, K (500°C), He, H_2 at h.t.	Bending strength 50,000 lb/sq.in. (room temperature)
UC_2	2400	10.6	20°C–0.08	Reacts with H_2O and air at l.t. Resistant to H_2, He at h.t.	
UN	2650	13.5		Complete reaction with O_2 at 510°C	
USi_3	1510	6.0		Good resistance to air up to 750°C	
ThO_2	3220		600°C–0.01 1200°C–0.008	Good resistance to all coolants at h.t.	Bending strength about 15,000 lb./sq.in.
ThC	2630				
PuO_2	~2240				

* h.t. = high temperatures (> 1,000°C); l.t. = low temperatures (< 300°C).

fuel cycle, thermal neutrons are used for fission; to maintain a chain reaction it is necessary that the ratio of neutrons produced to neutrons consumed (in propagating the chain reaction and in parasitic neutron capture) be greater than one. The use of any element with high thermal neutron cross section would be detrimental to the neutron economy of the system. A thermal utilisation factor, defined by the ratio

of neutrons absorbed by pure natural uranium to the number of neutrons absorbed by all the materials present is given by

$$f = \frac{N_1 (\sigma_a)_1}{N_1(\sigma_a)_1 + N_2(\sigma_a)_2 + N_3(\sigma_a)_3 + \ldots}$$

where

N_1 = number of uranium atoms per cm^3.
$(\sigma_a)_1$ = thermal neutron cross section of natural uranium, in barns.
N_2 = number of atoms of the element combined with U atoms, per cm^3.
$(\sigma_a)_2$ = thermal neutron cross section of the element combined with U, in barns.
$N_3 \cdots$ = number of atoms of moderator, coolant etc. in the system, per cm^3.
$(\sigma_a)_3 \cdots$ = thermal neutron cross section for the materials in question, in barns.

It is evident from the above equation that the uranium compound used as fuel should have a high U volume density and the combining element a low absorption cross section. C, Si, O, and to a lesser degree N, have low absorption cross sections (see Table II) and the compounds of uranium with these elements reasonably satisfy these requirements.

TABLE II

Parasitic absorption cross section for thermal neutrons of some elements

Element	m.p. (°C)	σ_a (barns)
O		0.0016
C		0.0045
Si		0.25
N		1.8
U	1132	3.5
Be	1280	0.009
Zr	1852	0.18
Nb	2468	1.1
Fe	1535	2.43
Mo	2620	2.5
Cr	1890	2.9
Cu	1083	3.6
Ni	1455	4.5

When a ionic solid is subjected to radiation, the neutrons and heavy charged particles may strike atoms in the crystal lattice, which are thus displaced to an interstitial position leaving a gap in the lattice. The displaced atoms may have sufficient energy to cause additional displacements in the lattice. When a fast charged particle passes through matter, a large amount of energy is dissipated at localised points in the lattice causing an increase in temperature above the boiling point of the material. Heat transfer from this small volume is rapid, since the bulk temperature

of the solid is normally close to room temperature and the vaporised material is immediately quenched by conduction. As a result the lattice is disturbed, and amorphous material or small crystal regions can be formed. (This phenomenon is known as thermal spikes). On account of these radiation effects, ceramics may be expected to decrease in density, thermal conductivity and strength[14]. Cubic lattices suffer less dimensional change, and radiation damage is less in solids having ionic bonds. Some of these changes may be reversed by annealing at high temperatures or may not take place at all at the temperature at which the ceramic fuel is irradiated.

Neutron irradiation causes a decrease in density and loss in crystallinity in quartz, and metastable phase transformations and lattice expansions in zirconia and barium titanate[15]. Decrease in thermal conductivity (30–80%) and density (0–3%) has been reported[16] for zirconia, mica, cordierite, fosterite, steatite, and the oxides of aluminium, titanium and beryllium. Small dimensional changes, or none, have been reported by Johnson[17] for a number of ceramic materials under irradiation. Most important in fuel elements are the fission products continuously accumulating as impurities in the parent lattice. Their damaging effect will depend on whether they are at least partially accommodated in the parent lattice, separate, or react with the original material. The few data available on ceramics subjected to fission fragments damage at high temperatures will be discussed below. Retention of fission products by ceramics is expected to be better compared with uranium, provided the materials used are near their theoretical density or have closed pores. The crystal lattices of the uranium ceramics under discussion are more open than the lattice of uranium and capable of interstitial accommodation of foreign atoms.

Corrosion resistance to coolants is expected to be much better in certain oxide ceramics than in uranium metal; it generally decreases in the following order: silicides, nitrides, carbides.

Ceramics are brittle, and generally possess low thermal conductivity and poor thermal shock resistance.

Ceramic fuel elements are made by cold pressing of the powder and subsequent sintering, or alternatively by hot pressing; high temperatures and protective atmospheres are entailed and fabrication costs may be higher compared with uranium metal elements. Efforts are being made to develop new and more economical processes. The compound most extensively investigated is uranium dioxide. It can be prepared by different methods[18,19], two of which have been used industrially:

1) Thermal denitration of uranyl nitrate hexahydrate $[UO_2(NO_3)_2 \cdot 6H_2O]$ to UO_3, followed by hydrogen reduction.

2) Hydrolysis of UF_6 with dilute ammonia solution to form a precipitate of ammonium diuranate, followed by pyrohydrolysis with steam at 800–850°C to U_3O_8 and finally reduction with hydrogen. This last method gave uranium dioxide with better sintering properties.

While the powder obtained by the first method must be compacted at 250,000 psi and sintered for 8 hours at 1675°C to obtain pellet densities of 93% to 95% of the

theoretical, the powder obtained by the second method is compacted at 40,000 psi and sintered at 1650°C for an hour to obtain the same density. It has been shown that the differences in behaviour of the two samples of uranium dioxide are due mainly to particle size differences.

The thermal conductivity or uranium dioxide is low, and is further reduced with increasing temperature (Table I), a fact which limits the size of fuel elements made of it; the pellets crack easily when subjected to thermal shock.

Very satisfactory results have been obtained with uranium dioxide under irradiation. Compacted and sintered uranium dioxide[20] showed no significant changes in diameter or length when irradiated to burn-ups to 10,000 MWD/T up and maximum central temperatures up to 2000°C. After irradiation the pellets are usually fragmented due to thermal stress. Uranium dioxide shows good retention of the fission products; pellets with an axial temperature of 1500°C released only 1.5% of the fission gases produced. Uranium dioxide has been irradiated as high as 50% fission of uranium atoms. The fuel performed satisfactorily and the swelling rate was lower than for any other known fuel system[21]. Another attractive feature of uranium dioxide is its corrosion resistance to mostcoolants used in power reactors (Table I).

Combinations of uranium dioxide with other oxides have been investigated to overcome some of the disadvantages of uranium dioxide. ThO_2-UO_2 dioxides could be sintered in air[22]. (Uranium dioxide cannot be sintered in air as it oxidises to higher uranium oxides which have less irradiation stability). Admixtures such as BeO and ZrO_2 show promise in increasing the thermal conductivity and fission gas retention. Some thermal conductivity data of different combinations are given in Figure 1.

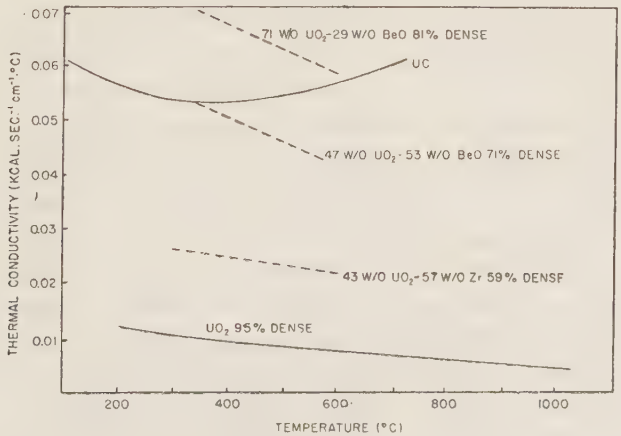

Figure 1

Thermal conductivity of some high-temperature fuels[28]

Uranium carbide is a refractory compound which has certain advantages over UO_2 (Table I). The bending strength of UC is three times that of uranium dioxide and its thermal conductivity is close to that of uranium. The thermal shock resistance of UC is reported to be much higher than that of uranium dioxide. No changes took place on repeated quenching from 1000°C to room temperatures, while samples of uranium dioxide cracked after three quenchings under these conditions[23,24].

No swelling of uranium carbide was noticed under irradiation[10], although release of 10% of the fission gases occurred after a burn-up of 3000 MWD/T at 630°C. Irradiation tests with arc-melted UC indicate that the fission gas release amounts to about 0.1% for irradiations up to 2000 MWD/T at 770°C, probably because of the lower porosity of the product. The sintering of UC powder (prepared either by reduction *in vacuo* of uranium dioxide at 1800°C, or by carburisation of uranium hydride at 650°C) is carried out between 1800–2000°C *in vacuo* or in argon to obtain 85% of the theoretical density. A new process, by which stoichiometric amounts of uranium and graphite powders are compacted under loads of 10–20 ton/sq.in. at 800°C, seems more attractive. The UC is obtained in a solid-state reaction with 85–90% of the theoretical density. Higher densities (up to 98% of theoretical) have been achieved by a similar technique[25], with sintering temperatures up to 1000°C. UC of 98% of the theoretical density could be prepared by a "drop casting" arc-melting technique, but this process is rather expensive[24].

Two other uranium compounds have recently aroused interest: uranium nitride, due to its high uranium density and high melting point, and uranium silicide (USi_3) due to its good resistance to oxidation in air.

Power reactors using ceramic fuels are listed in Table III.

CERMET FUEL ELEMENTS

A cermet is a combination of ceramics and metal, whose micro structure consists of sizeable ceramic particles and a continuous metallic matrix. The bond between the ceramic grain and metal may be due to wetting and to mutual partial solubilities.

The features of a cermet fuel element can be summarised as follows:

a) Localisation of radiation damage caused by the fission products around the fissile particle, leaving an uninterrupted and undamaged zone between the fissile particles. The average range of fission products is the distance that a recoiling fission product can penetrate into the non-fissile phase. More than twice this distance is needed between two fissile particles to leave an undamaged zone between them. Since the thickness of the damaged zone produced by fission products is constant for a specific matrix, reduction of the particle size of the fissile material increases the fraction of damaged matrix. It can be seen that increasing the volume fraction of the fissile particles also increases the fraction of damaged matrix. These relationships are schematically illustrated in Figure 2 for an idealised dispersion system[26].

TABLE III

Ceramic and cermet fuelled power reactors

Name and type of reactor	Ralng	Fuel characteristics	Coolant characteristics	Burn-up	Remarks
Shippingport (USA) Pressurised water reactor (PWR)	60 MW	UO_2 pellets, Zircalloy-clad	Water Outlet temp. 283°C	10,000 MWD/T	In operation since 1957
Zenith (UK) Prototype of HTGCR	100 W	UO_2-ThO_2 pellets in graphite tubes, temp. 800°C	Nitrogen Inlet temp. 400°C Outlet temp.* 950°C		Critical 1959
Dresden (USA) Boiling water reactor (BWR)	180 MW	UO_2 pellets, Zircalloy-clad	Water Inlet temp. 260°C Outlet temp. 282°C	10,000 MWD/T	Critical 1959
Exp. high temp. power reactor (Germany)	15 MW	UC-ThC in graphite (pebble bed reactor)	Helium-neon mixture Outlet temp. 600–1000°C		Critical 1961
Advanced gas cooled reactor (UK)	28 MW	UO_2 pellets Be-clad	Gas Inlet temp. 300°C Outlet temp. 550°C	8,000 MWD/T	Critical 1961
Army packaged power reactor (APPR) (USA)	10 MW	UO_2 dispersed in stainless steel	Water Inlet temp. 220°C Outlet temp. 232°C		In operation

* Outlet temperature from heater to simulate conditions of actual operation.

b) Considerable improvement in mechanical, thermal and corrosion properties can be obtained by the use of cermets instead of pure ceramics[27]. These are quantitatively illustrated in Figures 3 and 4.

c) The use of cermet fuel elements would entail a further increase of parasitic absorption of neutrons. Some metals which can be considered for the matrix are listed in Table II; metals with relatively high cross sections like Ni, Fe, Cr might be used in reactors using enriched uranium as fuel.

d) Fabrication costs of cermet fuel elements compared with ceramic elements can be reduced, if the sintering temperatures and times can be decreased.

e) A chemical reaction between the ceramic particle and the metal matrix may take place during fabrication, or later in service. It is obvious that if any such reaction takes place the resulting phases may completely alter the characteristics of the system. If, for instance, in the system uranium carbide–nickel the reaction

$$UC + 5Ni = UNi_5 + C$$

takes place, it is evident that the properties of new combination ($UNi_5 + C$) will be entirely different from those of the original UC + Ni; in addition, the refractory properties of UC will be lost. It is therefore necessary to determine accurately the compatibility of the phases involved.

A number of dispersed fuel combinations have been investigated[26, 28]; the most promising combinations seem to be: UO_2-Mo, UO_2-Nb, UO_2-stainless steel, UC-C, UC_2-C, UBe_{13}-Be.

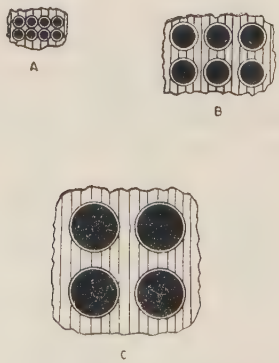

Figure 2
Damaged matrix zones for a constant volume fraction dispersant[26]

LEGEND

	A	B	C
Particle size (μ)	35	105	210
Spacing of damaged zones (μ)	0	24	60

Volume fraction of particles = 20%

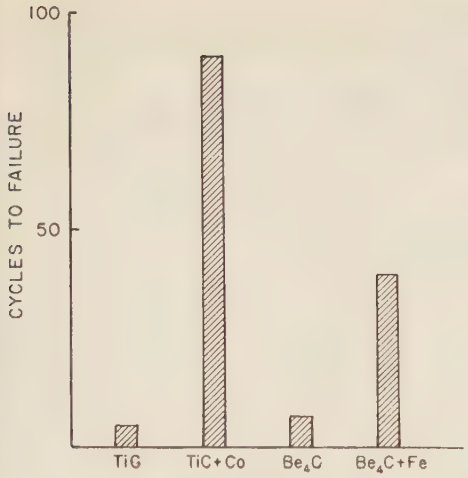

Figure 3
Improvement in thermal shock resistance by addition of metal[27]

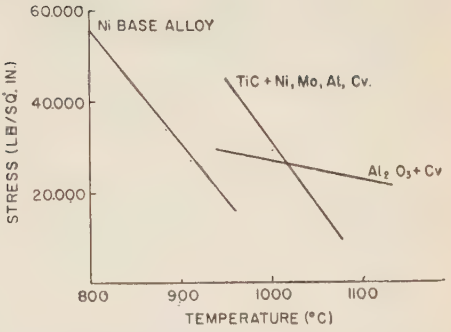

Figure 4
Comparison of stress rupture strength of cermets and alloys[27].

CONCLUSIONS

The use of ceramic and cermet fuel elements offers the possibility of overcoming the temperature and burn-up limits inherent in metallic uranium elements. Ceramics and cermets, however, have their own problems to which solutions must be found. Investigations and performance data already available give promising indications.

REFERENCES

1. Grainger, L., 1958, *Uranium and Thorium*, G. Newnes, London.
2. Wooton, K. J. and Dennis, W. E., 1958, *Proc. Int. Conf. on Peaceful Uses of Atomic Energy*, **6**, 362.
3. Data Sheet on World Reactors, 1959, *Nuclear Eng.*, **4**, 338.
4. UKAEA, 1959, 5th Annual Report.
5. Banks, W. S., 1959, *Nucleonics*, **17**, 96.
6. Israeli AEC, 1955, *Proc. Int. Conf. on Peaceful Uses of Atomic Energy*, **1**, 192.
7. Hayward, B. R., 1959, *Nucleonics*, **17**, 14.
8. Bochvar, A. A. and Thomson, G. I., 1959, *Reactor Tech.*, **1**, 47.
9. Englander, M., 1958, Report CEA-776.
10. Murray, P. and Williams, J., 1958, *Proc. Int. Conf. on Peaceful Uses of Atomic Enrrgy*, **6**, 538.
11. Stohr, C. E. and Leavy, E. A., 1958, *Ibid.*, 324.
12. Lacy, C. E. and Leavy, E. A., 1958, Report KAPL–1952.
13. Boudouresques, M. B. and Englander, M., 1959, *Progress in Nuclear Energy*, Series 5, **2**, 621, Pergamon Press, London.
14. Livey, D. T., 1957, *Trans. Brit. Ceramic Soc.*, **56**, 482.
15. Crawford, J. H. Jr., 1959, *Progress in Nuclear Energy*, Series 5, **2**, 531, Pergamon Press, London.
16. Bopp, C. D. *et al.*, 1956, Report TID–7530, 66.
17. Johnson, J. R., 1956, *Journ. of Metals*, **8**, 660.
18. Belle, J., 1958, *Proc. Int. Conf. on Peaceful Uses of Atomic Energy*, **6**, 569.
19. Runnals, O. J. C., 1959, *Nucleonics*, **17**, 104.
20. Robertson, J. A. L., *et al.*, 1958, *Proc. Int. Conf. on Peaceful Uses of Atomic Energy*, **6**, 655.
21. Barney, W. K., 1958, *Ibid.*, 677.

22. Kittel, J. H. and Handwerk, J. H., 1958, Report ANL–5675.
23. Boettcher, A. and Schneider, G., 1958, *Proc. Int. Conf. on Peaceful Uses of Atomic Energy*, **6**, 561.
24. Secrest, A. C., *et al.*, 1959, Report BMI–1309.
25. Dubuisson, J., *et al.*, 1958, *Proc. Int. Conf. on Peaceful Uses of Atomic Energy*, **6**, 551.
26. Weber, C. E., 1959, *Progress in Nuclear Energy*, Series 5, **2**, 295, Pergamon Press, London.
27. Deutsch, G. C., *et al.*, 1958, Report AGARD–185.
28. Strasser, A., 1959, Report HaP–2818.

CRITICAL EVALUATION OF THE CYANIDIN REACTION FOR FLAVONOID COMPOUNDS

A. KWIETNY* AND J. B. S. BRAVERMAN

Division of Food- and Biotechnology, Technion–Israel Institute of Technology, Haifa

ABSTRACT

A detailed study was made of the so-called cyanidin test for the determination of total bioflavonoids, expressed as hesperidin. The various factors affecting this reaction have been investigated, such as: the choice of blank for comparison, changes in hesperidin solutions on standing in contact with air, the influence of ethanol and acid concentrations on the cyanidin colour and the important role of magnesium, which is apparently not restricted solely to the formation of nascent hydrogen.

Recently, much interest has been focussed on certain flavonoid plant compounds, especially on several apparently possessing biological activity and known as bioflavonoids. Appreciable quantities of some of these are now produced industrially.

Among the various methods used for qualitative and quantitative estimation of flavonoid substances, such as flavons, flavanones and flavonols, the cyanidin test is the most general. Willstätter[1] in 1914 was the first to suggest this test, based on a colour reaction between a colourless (or pale yellow) solution of a flavonoid compound and an ethanol-HCl mixture in the presence of a strip of magnesium. Since then, several authors have described the cyanidin reaction[2,3,4,5,6], and Sunkist Growers Laboratories have recently developed a quantitative method based on it, published as a leaflet[7]. In this reaction, the colour of the solution under investigation changes to red, red-violet or magenta. The absorbance of the coloured solution can be measured in light of appropriate wavelength and the amount of the flavonoid compound estimated accordingly.

However, although the cyanidin reaction is extremely convenient for both qualitative and quantitative determination of bioflavonoids, in practice it does not always ensure quantitative reproducibility, owing to a number of factors affecting it.

In the present work an attempt was made to study these factors and conditions as well as the properties of the coloured solutions obtained.

---

* Part of a thesis submitted in partial fulfilment of the requirements for the M.Sc. degree.

Received December 17, 1959

MATERIALS, METHODS AND EQUIPMENT EMPLOYED

The flavanone used was hesperidin, prepared from orange peel and purified by repeated crystallisation from NaOH and formamide (according to the methods described by Hendrickson and Kesterson[8] and Pritchell and Merchant[9]) to give consistently a melting point of 262°C.

Cyanidin reactions were carried out in a test tube placed in an ice bath, the medium consisting of 4 ml hesperidin solution (usual concentration 0.1—1.0 mg/ml) in 0.01N NaOH, 145 mg Mg (in the form of ribbon strips, 3 mm width, 0.16 mm thickness) and 6 ml ethanol (95%) – HCl (conc., sp. gr. 1.18) mixture, 2:1 v/v. On completion of the Mg-HCl reaction the test tube was removed from the ice bath and time allowed for the colour to develop.

Absorbances of the coloured solutions were then determined by means of a DU Beckman spectrophotometer (Model 2400) at 560 mμ against a distilled water blank, using 10 mm cells.

EXPERIMENTAL

Choice of blank and wavelength. Conformity with Lambert-Beer law.

The medium used for determining the most suitable blank consisted of 4 ml hesperidin solution (0.3 mg/ml) in 0.01N NaOH, 145 mg Mg and 6 ml ethanol-HCl mixture, the colour being allowed to develop for two hours. Three blanks were tested, as follows:

(a) solution prepared as above (recommended by Sunkist Growers Laboratories[7]) but without magnesium,

(b) solution prepared as above, but without hesperidin,

(c) distilled water.

The results of the spectrophotometric measurements are shown in Figure 1. Identical

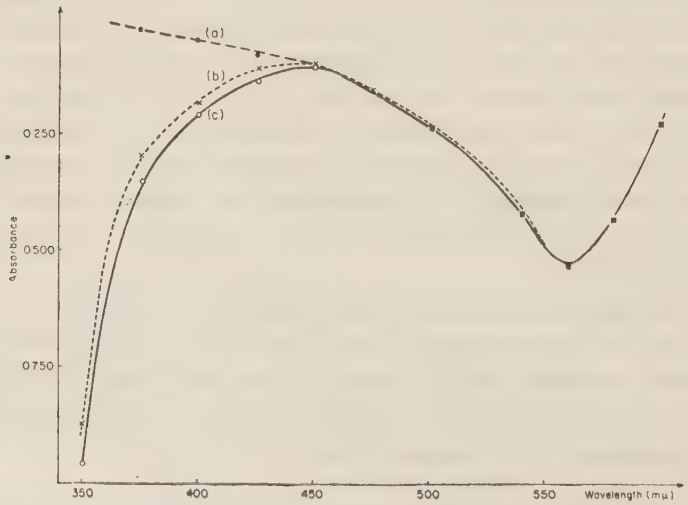

Figure 1

Cyanidin colour measured against various blanks. (a) Solution without magnesium. (b) Solution without hesperidin. (c) Distilled water.

results were obtained in all three cases at 450–600mμ; the maximum in the absorbance spectra corresponds to 560mμ. It can be assumed, therefore, that there is no need for a complex mixture and a distilled water blank would be satisfactory. The blank recommended by Sunkist Growers Laboratories may actually lead to erroneous results, in view of the fact that at 350 mμ (as used by them) its absorbance would be higher than that of the solution.

The conformity obtained with the Lambert-Beer law is illustrated in Table I.

TABLE I

Hesperidin solution (mg/ml)	Absorbance	
	1st series	2nd series
1/2	0.840	0.812
1/4	0.432 (0.420)	0.410 (0.406)
1/6	0.274 (0.280)	0.267 (0.271)
1/12	0.136 (0.140)	0.133 (0.135)

(Figures in brackets — theoretical values according to Lambert-Beer law)

In each series, the medium consisted of 4 ml of one of the hesperidin solutions, 145 mg Mg and 6 ml ethanol-HCl mixture. Readings were taken at 560 mμ one hour after completion of the Mg-HCl reaction.

Development of cyanidin colour

From Figure 2 it is clearly seen that the colour intensifies during the first 3 hours after completion of the Mg-HCl reaction and subsequently fades. Here the wavelength used was 560 mμ.

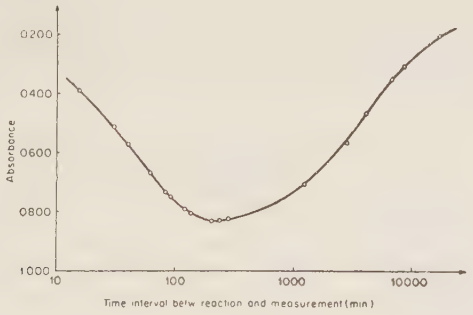

Figure 2
Development of cyanidin colour. (Absorbances measured at 560 mμ).

The behaviour of the cyanidin colour (prepared from a 0.5 mg/ml hesperidin solution) on standing in light and in the dark is illustrated in Figure 3. It appears that in all cases the maximum shifted with time from 560 mμ to 500 mμ. 15 days' standing appreciably reduced the absorbance.

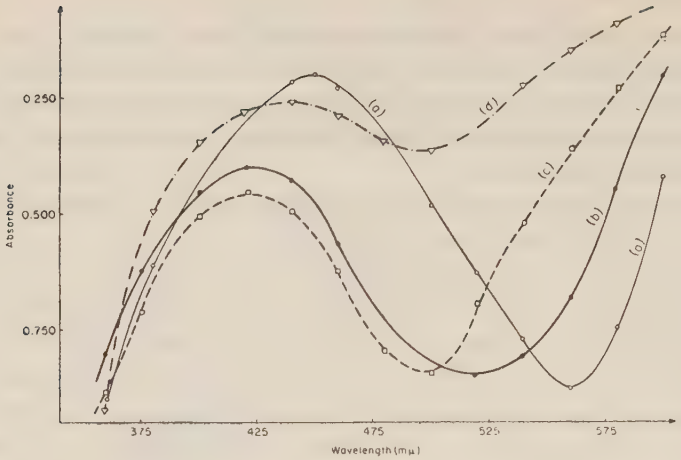

Figure 3

Behaviour of cyanidin colour on standing. (a) 2 hrs. after completion of reaction. (b) After 5 days' standing in the dark. (c) After 5 days' standing in transparent glass container. (d) Same as (c), after 15 days' standing.

In order to determine the effect of standing on the hesperidin solutions, cyanidin reactions were carried out in the same solution at regular intervals. In all cases, the medium consisted of 4 ml hesperidin solution (0.4 mg/ml) in 0.01N NaOH, 145 mg Mg and 6 ml ethanol-HCl mixture. Results are given in Figure 4, in which solid lines represent absorbances of the same solution measured after successive intervals of standing, and dashed lines those of different solutions measured at equal intervals after completion of the Mg-HCl reaction, the numbers denoting time in days. Thus line 0 refers to the colour obtained from the fresh hesperidin solution, line 1 — to that obtained from a solution after one day's standing, and so on.

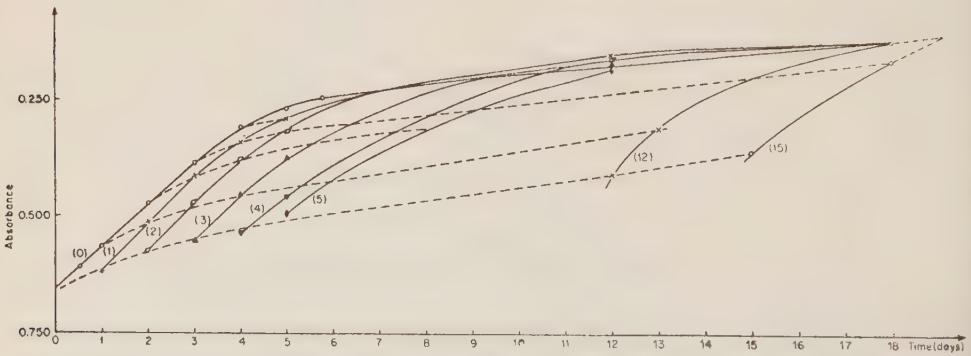

Figure 4

Effect of standing on hesperidin solutions. (Absorbances measured at 560 mμ). Solid lines — same solution after successive intervals of standing. Dashed lines — different solutions at equal intervals after completion of reaction. (Numbers denote time in days).

The conclusions are:

(a) The fresher the hesperidin solution, the higher the absorbance of the colour obtained.

(b) The colour tends asymptotically to a stable limit.

As the colour changes on standing, the maximum shifts from 560 mμ to 500 mμ as shown in Figure 3; colours obtained from old hesperidin solutions, although lower in absorbance, retained their maximum at 560 mμ (see Figure 5).

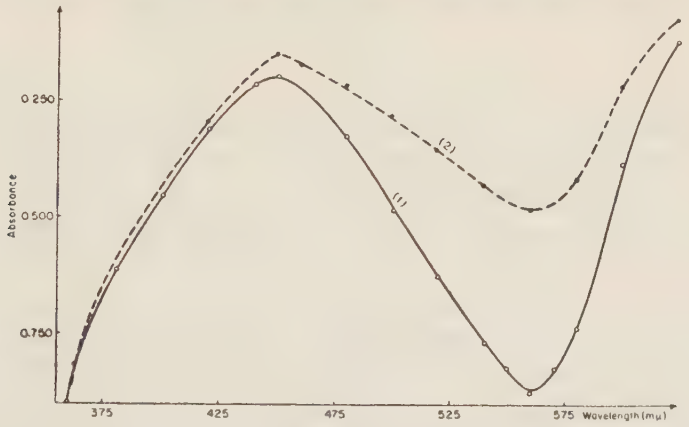

Figure 5

Cyanidin colour prepared from fresh and old hesperidin solutions.
(1) Fresh. (2) Old.

In an additional series, cyanidin reactions were carried out in three samples of a special hesperidin solution (0.178 mg/ml; *p*H 10.2) of which the first was stored in a desiccator under vacuum for 12 days, the second — for the same period in a closed transparent glass container, half-full, and in the third the reaction was carried out immediately on preparation. The medium consisted of 2 ml hesperidin solution mixed with 2 ml 0.01N NaOH, 145 mg Mg and 6 ml ethanol-HCl mixture, and absorbances were measured 2 hours after completion of the Mg-HCl reaction. Results are shown in Table II.

TABLE II

Conditions of storage	Absorbance
Fresh	1.132
Under vacuum	1.030
In contact with air	0.702

There is thus reason to believe that hesperidin in solution changes on standing, and the cyanidin reaction involves the unchanged part. It appears that contact with air plays an important role in the process, but no attempt was made in this case to elucidate its nature.

The nature and behaviour of the cyanidin colour

It used to be generally accepted that, under the conditions of the cyanidin reaction, the flavanone is transformed into a pyrylium salt [1,2,3,6]. The change in the molecular skeleton was suggested to be as follows:

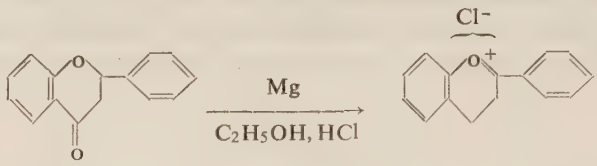

However, Geissman[10] holds that the compounds formed in the cyanidin reaction are not pyrylium salts. His view is based on the following facts:

(a) The red colours produced in the cyanidin reaction are unstable while pyrylium salts (such as anthocyanins) can be stored for considerable periods without affecting the colour.

(b) A very high concentration of acid is required for the development of the colour; if the solution is insufficiently acid, marked fading takes place. (Anthocyanins, on the other hand, do not change even when stored at higher *p*H).

To settle this controversy, a number of experiments were carried out, in which the influence of the water/ethanol/acid proportions on the cyanidin colour was investigated.

Figure 6 shows the changes in absorbance measured at 560 mμ at various intervals after the Mg-HCl reaction. The solid line represents absorbances in a reaction between 4 ml hesperidin solution (0.5 mg/ml) in 0.01N NaOH, 145 mg Mg and 6 ml

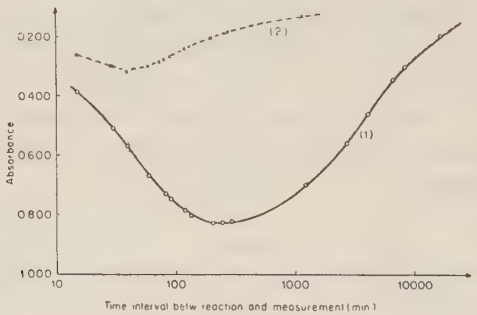

Figure 6

Influence of water/ethanol/acid proportions on cyanidin colour. (Absorbances measured at 560 mμ). (1) Ethanol-containing solution. (2) Aqueous solution.

ethanol (95%)–HCl (conc.) mixture, 2:1 v/v; the dashed line represents a parallel series in which the ethanol was omitted, the acid solution consisting of a 2:1 v/v

water-HCl mixture. It appears that the presence of ethanol favours higher intensity; spectra also differ, as is clearly seen from Figure 7.

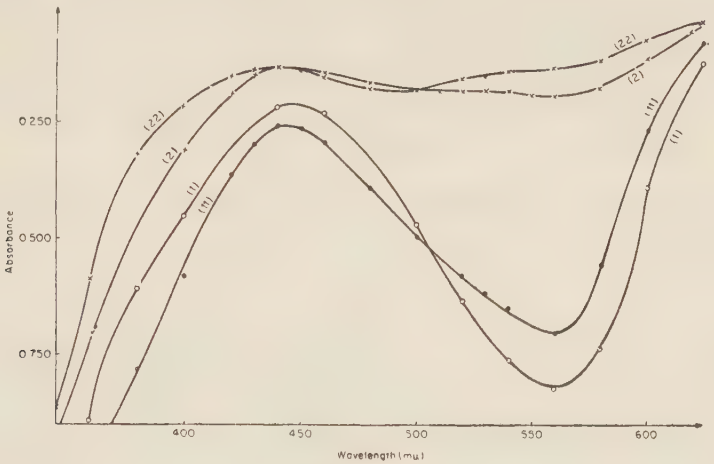

Figure 7

Development of cyanidin colour in ethanol-containing and aqueous solutions. (1) Ethanol-containing solution, 2 hrs. after completion of reaction. (11) Same as (1), 24 hrs. after completion of reaction. (2) Aqueous solution, 2 hrs. after completion of reaction. (22) Same as (2), 24 hrs. after completion of reaction.

To determine the dependence of the cyanidin colour on acidity a series of reactions was carried out in a medium consisting of 4 ml hesperidin solution (1 mg/ml) in 0.01N NaOH, 130 mg Mg and 6 ml of one of the acid solutions as shown below. Results are given in Table III.

TABLE III

Sample No.	6 ml of acid sol. made up of: ethanol-HCl (conc.) 2:1 v/v (ml)	ethanol-water 2:1 v/v (ml)	Colour	Absorbance at 560 mμ	*pH*
1	6	—	Deep red	1.356	Off scale
2	5	1	Deep red	1.520	Off scale
3	4	2	Deep red	1.690	Off scale
4	3	3	Pink-yellow	0.103	6.7
5	2	4	Colourless	0.085	8.8
6	1	5	Colourless	0.35	8.8

It seems that the colour disappears if the *p*H is not low enough.

In an additional series on the influence of the water/ethanol/acid proportions on the cyanidin colour the medium consisted of 25 ml hesperidin solution (0.5 mg/ml) in 0.01N NaOH, 900 mg Mg, 18.8 ml ethanol, 9.4 ml HCl (conc.) and 9.4 ml water. 2 hours after completion of the Mg-HCl reaction eight samples of the medium were placed in test-tubes, as follows:

Sample 0 : 10 ml
Samples 1—7: 5 ml each.

Of these, samples 1—7 were diluted with 5 ml of one of the following solutions, as shown in Table IV.

TABLE IV

Sample No.	Composition of diluent		
	Water (ml)	ethanol (ml)	HCl (conc.) (ml)
1	5.0	—	—
2	2.5	—	2.5
3	—	2.5	2.5
4	—	5.0	—
5	2.5	2.5	—
6	—	—	5.0
7	1.67	1.67	1.67

Both original and diluted media were measured at 560 mμ immediately after dilution and subsequently over a number of days. Results are given in Figure 8.

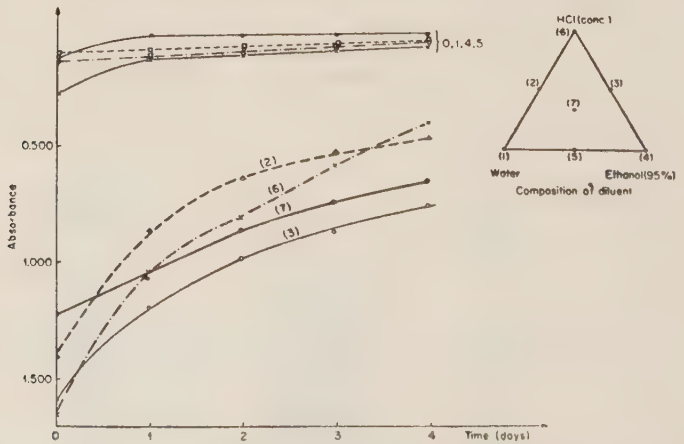

Figure 8

Influence of water/ethanol/acid proportions on cyanidin colour in diluted solutions. (Absorbances measured at 560 mμ).

It appears that the colour is highly intensified when diluted with acid solutions, ethanol-containing solutions intensifying it more strongly than aqueous solutions.

Attention was focussed on the special role played by magnesium in the formation of the cyanidin colour. This role is not restricted to providing nascent hydrogen; in fact, when equivalent amounts of zinc powder, aluminium powder and sodium were substituted for magnesium the characteristic cyanidin colour failed to form, but appeared the moment Mg was added.

SUMMARY

Accurate results are obtained when solutions of pure hesperidin are analysed by the cyanidin method.

Estimation is convenient and rapid owing to close conformity with the Lambert-Beer law, and the spectrophotometric absorbance measurement (at 560 mμ-wavelength, against a blank of distilled water) should be carried out simultaneously with that of a solution of known concentration; this is because of a very large variety of factors governing the development of the cyanidin colour and thus precluding the use of standard curves.

Hesperidin solutions undergo changes on standing: cyanidin reactions in fresh solutions give higher absorbances than those prepared from the same solutions after standing. The change is even more marked when stored in contact with air.

The development of the cyanidin colour is a function of time: maximum absorbance is reached within about 3 hours after completion of the Mg-HCl reaction and subsequently decreases asymptotically, tending to a constant limit.

Increase of ethanol and/or acid content intensifies the cyanidin colour; exposure to a non-acid environment results in disappearance of the colour. The spectra of ethanol-containing solutions differ markedly from those of aqueous solutions.

Magnesium plays an important role in the formation of the red colouring substances, not restricted to providing nascent hydrogen.

ACKNOWLEDGMENT

The authors express their indebtedness to Dr. G. Zimmerman of this Division for his valuable advice and criticism.

REFERENCES

1. WILLSTÄTTER, R., 1914, *Berichte der Deutschen chemischen Gesellschaft*, **47**, 2865–74.
2. LINK, K. P., 1944, Anthocyanins and flavons, *Organic Chemistry* (ed. H. Gilman), Vol. 2, pp. 1315–1340, John Wiley, New York.
3. FIESER, L. AND M., 1956, *Organic Chemistry*, 3rd ed., pp. 821–824.

4. Geissman, T. A., 1955, Anthocyanins, chalcones, aurones, flavones and related water soluble plant pigments, in *Modern Methods of Plant Analysis* (ed. K. Paech and M. V. Tracy), Vol. 3, pp. 450–498, Springer, Berlin.
5. Linskens, H. F., 1955, *Papierchromatographie in der Botanik*, pp. 202–220, Springer, Berlin.
6. Birch, A. J., 1957, Biosynthetic relations of some natural phenolic and enolic compounds, in *Progress in the Chemistry of Organic Natural Products*, Vol. 14, pp. 186–217, Springer, Vienna.
7. Sunkist Growers Laboratories, 1955, *Analytical Methods for the Citrus Bioflavonoid Products*, Sunkist Growers Products Dept., Ontario, California.
8. Hendrickson, R. and Kesterson, J., 1956, Crude hesperidin purification, *The Citrus Industry*, **37**, No. 1, 7.
9. Pritchell, D. E. and Merchant, H. E., 1946, The purification of hesperidin with formamide, *J. Am. Chem. Soc.*, **68**, 2108.
10. Geissman, T. A. and Clinton, R. O., 1946, The colored reduction products of polyhydroxyflavanones, *J. Am. Chem. Soc.*, **68**, 700.

BLACK POINTED WHEAT

Y. Pomeranz
Food Laboratory, Ministry of Commerce and Industry, Haifa

ABSTRACT

Wheat varieties grown in Israel were shown to have different susceptibility to black point discolouration. The milling of a wheat grist containing up to about 13% black point kernels caused no deterioriation in flour colour—at low and medium extraction—as well as ion water absorption, dough handling properties and bread quality. Black point kernels showed slightly decreased viability, but no significant increase in mould count and fat acidity—as compared with sound wheat.

The description 'black pointed wheat' applies to a discolouration of the outer bran of the grain, mainly covering the embryo and partly extending over the cheeks.

The discolouration is thought to be of fungal origin[1] and to occur when the chaff surrounding the grain becomes wet due to late rain, the germ tip being the last part to be freed from moisture.

It has been stated in discussing the black point disease of wheat that the infection was caused by *Alternaira* spp., which, nevertheless, has no deleterious effect on the value of the grain for feeding purposes[2]. Kent-Jones and Arnos[3] attribute the fungal disease of wheat known as black point to the infection of the grain with a species of *Helminthosporum*. Flours milled from the wheat exhibiting "black point" examined by the authors possessed normal baking quality.

This type of damage should be distinguished from "sick" wheat which is identified by profound brown to black discolouration of the whole germ and accompanied by high mould count, high fat acidity values, low viability and poor bread baking quality. Several investigators have shown "sick wheat" to be associated with mould growth. Thomas[4] believed "sick" wheat to be grain which has lost its viability through toxic products secreted by moulds.

Milner et al.[5] found *Aspergillus glaucus* and *A. flavus* to be the most abundant in "sick" wheat kernels, whereas *Alternaria* was most prevalent in sound wheat. Some of the literature indicates that "sick" wheat can develop under conditions where moulds grow with difficulty and when mould growth is inhibited by chemical preservatives.

The term "sick" wheat is rather poorly defined and though usually confined to damaged wheat which has been stored in large quantities under unfavourable conditions, the term is sometimes applied to freshly harvested wheat. In this case, its occurrence is thought[6] to be associated with conditions which kill the germ after it has been partly germinated.

Received February 19, 1959

The occurrence of "sick" wheat is considered undesirable in milling as it results in flour of poor colour[7]. Green and Stewart reported[8] that the presence of wheat showing discoloured pericarp affected the grade colour of 72% commercially milled flour. The patchwise disolouration of the grain skin was traced to the development of mycellium of *Cladosporium* spp. The fungal growth was confined to the outer layer of the kernel and has not penetrated into the aleurone and endosperm. The poor colour of the flour was attributed to excessive fracturing of bran during milling.

The present study was undertaken to investigate the occurrence of black point in local wheat and its influence on milling and bread baking quality.

MATERIALS AND METHODS

Source of wheat: Samples of 8 varieties of local wheat from the 1956, 1957 and 1958 yearly crops were tested.

Detection of damaged wheat: The detection of black point wheat was made on visual examination of the kernels. The percentage of damaged wheat was determined by weighing germ discoloured kernels picked out from about 50 g of seed.

Viability tests: Two hundred seeds were placed on wet blotting paper in trays kept at room temperature for 7 days. The seeds which had normal sprouts were considered viable.

Milling characteristics: The wheat was dampened to 15.5% moisture, tempered overnight and milled on a Buehler laboratory mill. Throughout the course of the investigation the milling conditions, i.e. setting of rolls, rate of feed, etc. were kept uniform in order to reveal any differences in milling characteristics due to mould growth. Though effort was made to maintain uniform milling, some minor variations in grinding are inevitable and though they are believed to be small, they must be considered when interpreting flour and bread quality data. Yields of flour are reported as percentage of the milled—total—products.

Moisture contents: A 10 g sample was heated—for $1^1/_2$ hours in the case of wheat, and 1 hour in the case of flour—in a semiautomatic Brabender oven at 130°C.

Fat acidity was determined by the method of Zeleny and Coleman[9].

Mould counts were made by the procedure outlined by Christensen[10]. (Moisture fat, fat acidity and mould count determinations were made on wheat ground through a 30 mesh sieve—in a Micropulverizer.)

Ash was determined on a 5 g sample incinerated overnight at 580°C in a silica crucible.

Protein was determined on a 1 g sample by the method outlined in Cereal Laboratory Methods[11].

Flour colour was measured with the Kent-Jones and Martin Colour Grader[12].

The *test weight* determinations were made with an Avery Apparatus.

Farinograms were obtained by mixing 50 g of flour in a small bowl (64 r.p.m. drive) for 15 minutes with distilled water to give maximum dough consistency centered about 500 Brabender unit line. Farinograph absorption is reported as the amount of water which was added to a flour (14% moisture basis) to give the mentioned consistency. Dough development time was read off from the Farinograph curves.

For *Extensograph curves* doughs were made from 300 g flour, 6 g salt and the amount of distilled water found from the Farinograph absorption test, less 3.0 percentage units to compensate for the added salt. This series of experiments was made on a commercially milled, untreated bakers' long patent flour. The doughs were mixed for 1 minute in a large Farinograph bowl, rested for 5 minutes and remixed until the curve was centered about the 500 unit line. Curves were drawn for duplicate 150 g doughs after 45, 90 and 135 minutes' rest periods

Baking tests: The straight dough method was employed in the baking tests and doughs were of such size as to yield commercial loaves of 500 g. The formula for the dough included flour, water, 3% compressed yeast and 1% salt (both percentages on flour basis); the dough was mixed in a Junior Hobart Mixer for 5 minutes at medium speed. Moulding was done by hand and optimum absorption was determined by the operator. Fermentation time varied between 90 and 105 minutes. Proof was kept constant at 75 minutes.

Starch liquefying properties were determined with the Amylograph by the method of Anker and Geddes[13].

RESULTS

Data presented in Table I show occurrence of black point on local wheat varieties.

TABLE I
Susceptibility of local wheat varieties to black point disease

Variety	Predominant class	1956 year crop		1957 year crop		1958 year crop	
		No. of samples tested	% of damaged samples	No. of samples tested	% of damaged samples	No. of samples tested	% of damaged samples
C.C.C. (var. *graecum*)	Soft white	174	22.6	593	4.2	56	—
Florence Aurore (var. *albidum*)	Semi hard	517	3.5	1973	2.3	61	—
Giza 4 (var. *melanopsus*)	Durum	373	5.6	276	37.3	—	—
Giza 50 (var. *melanopsus*)	Durum	3	—	7	12.5	22	9.0
Debia (var. *horano-leucomelan*)	Durum	4	—	6	—	2	—
Zenati Bouteille (var. *leucurum*)	Durum	227	1.8	438	17.1	40	27.5
Ethith (var. *horano-leucurum*)	Durum	3	—	2	—	4	—
Noorsi (var. *leucurum*)	Durum	298	0.7	583	2.7	31	—

Examination of data in Table I shows clear varietal differentiation in susceptibility of wheat to black point; black point—similar to "sick" wheat occurrence seems to be more prevalent in years when damp harvest conditions are encountered.

The extent of damage to the grains is given in Table II.

TABLE II

Comparison of viability, mould count and fat acidity of wheat kernels

Description of sample		Germination (%)		Mould count*		Fat acidity**	
		Sound	Damaged	Sound	Damaged	Sound	Damaged
Mixed Crop	1956	93	80	170	450	16.5	18.0
Noorsi	1957	63	61	600	520	15.8	18.6
Noorsi	1957	67	49	120	1750	—	—
C.C.C.	1957	95	93	4200	2940	21.3	24.1
C.C.C.	1957	90	95	3200	3200	26.4	28.0
Gizah IV	1957	84	88	735	560	17.9	20.2
Gizah IV	1957	79	81	520	1500	—	—
Zenati Bouteille	1957	95	90	210	1300	17.9	17.9

* Colonies per gram

** mg KOH per 100 gram wheat–dry matter basis

The number of fungi generally present on sound cereal grains is about 1000–2000 per gram (although smaller numbers were also given); above 50,000 moulds are reported on sick wheat[14].

Freshly harvested wheat of unquestionable soundness has normally fat acidity values between 10 and 20, whereas deteriorated wheat usually attains values above 50.

Results summarised in Table II must be interpreted with caution. Picking out of damaged kernels on visual examination is empirical and does not enable the distinction between different degrees of damage and the ascertaining of early stages of discolouration. Up to 50% of surface-sterilized (immersed for 1 minute in a dilute solution of mercuric chloride and rinsed in sterile water), apparently sound kernels, picked out from mixed parcels, when kept on a salt–malt–agar medium, for 3–5 days, showed signs of germ discolouration.

Practically no such darkening was observed in kernels from completely sound wheat parcels. Notwithstanding these limitations, it can safely be stated that the damage to the grains as assessed by germination, mould count and fat acidity was low, and did not entitle the damaged kernels to be termed "sick". "Sick" wheat

germs—observed upon removal of the bran layers which cover it—show a profound discolouration. No such darkening was observed on examination of black point wheat germs examined with a stereoscopic microscope, under a magnification of 20, after removal of pericarp.

Sound kernels—surface sterilized—were immersed in a malt-salt broth in which germs removed from surface sterilized kernels were kept for 5 days. The kernels were plated on an agar–malt–salt medium and incubated up to 5 days.

Kernels submerged in broth containing germs from sound seed showed no fungal growth; germs from apparently sound wheat caused microbiological growth in about 40% of the cases and immersing grain in broth containing black tip germs caused strong growth around all kernels. From the pericarp of black point wheat *Alternaria* spp. was isolated.

Deterioration of colour or bread baking potentialities of flour milled from sick wheat was not observed on milling Hard Red Winter wheat containing up to 10% black tipped durum wheat kernels—on a laboratory experimental mill to a relatively low extraction.

These data are summarized in Table III. Data in Table IV refer to milling tests made on sound or partly damaged local, soft wheat.

TABLE III

Characteristics of wheat flour

No.	Description of wheat	Total Extrac. (%)	White flour* Extrac. (%)	White flour* Grade (colour)	Dark flour** Extrac. (%)	Dark flour** Grade (colour)	Loaf volume*** (cc)
I	Hard Red Winter	68.5	52.6	4.2	15.9	8.2	1875 (av.)
IA	Hard Red Winter	68.7	51.5	4.4	17.2	9.2	
2	Added 4% sound	66.7	50.0	4.1	16.7	8.1	1750
3	Added 4% black point kernels	66.1	48.3	3.9	17.8	7.3	1725
4	Added 10% sound kernels	66.4	49.2	3.9	17.2	9.0	1800
5	Added 10% black point kernels	64.7	45.8	4.3	18.9	9.1	1800

* First and second reduction flours.

** Break (first, second and third) and third reduction flours (All extraction rates calculated as percentage of total milled products).

*** 500 g loaf-baked from mixture of break and reduction flour.

TABLE IV

Effect of presence of black pointed wheat kernels on bread baking quality of local soft wheat flour

Property	Wheat Variety			
	Florence Aurore		C.C.C.	
Wheat				
Percentage of damaged kernels (%)	—	12.7	—	11.7
Flour				
Ash (%)	0.50	0.48	0.55	0.54
Farinograph curves				
Absorption (%)	70.0	68.2	66.1	64.3
Development time (min.)	2.5	2.0	2.0	1.5
Extensograph curves				
Length (cm)	12.5	13.5	11.5	11.5
Height (B.U.)	650	620	620	640
Height at 5 cm (B.U.)	505	440	540	530
Amylograph data				
Height (max. viscosity B.U.)	680	560	690	560
Bread				
Loaf volume (ml)	1650	1700	1500	1475

Impaired baking quality, loaf volume and loaf texture,—characteristic of "sick" wheat flour—were not noted on addition of flour milled from black tipped wheat.

A slight improvement observed in loaf texture and crust colour in loaves No. 2 and 3 (Table III) should be attributed to the presence of small amounts of durum wheat flour.

The loaves described in Table III showed no differences in crumb colour. Minor variations in flour colour were probably caused by differences in extraction rate. Similarly, the presence of black pointed kernels in local soft wheat had little influence on the milling and bread baking quality of wheat as illustrated in Table IV.

The addition of whole meal wheat (sound and black pointed) prepared on a laboratory Micropulverizer—caused changes in colour of flour as reported in Table V.

Though the results in Table V cannot be directly extrapolated, they are suggestive as to the influence of black tipped wheat on high extraction flour.

TABLE V

Effect of wholemeal addition on grade colour of long patent flour

Addition of whole meal %	Sound wheatmeal	Black point wheatmeal
None	4.4	4.4
1	4.5	4.9
3	5.3	5.7
5	5.8	6.2
10	6.7	8.1

REFERENCES

1. Anonymous, 1954, *Bulletin of the Research Association of British Flour Millers*, **5,** 106.
2. Hansen, E. H. and Christensen, J. J., 1953, *Minnesota Agricultural Experimental Station, Technical Bull.* **206,** 1.
3. Kent Jones and Amos, *Modern Cereal Chemistry*, Northern Publ. Co., Liverpool, 5th ed., p. 520.
4. Thomas, R. C., 1937, The role of certain fungii in the "Sick-Wheat" problem, *Ohio Agricultural Expt. Station Bulletin*, **22,** 43.
5. Milner, M., Christensen, C. M. and Geddes, W. F., 1937, Grain Storage Studies V. Chemical and microbiological studies on "Sick" wheat, *Cereal Chem.*, **24,** 23.
6. Milner, M. and Geddes, W. F., 1954, Respiration and Heating, in: *Storage of Cereal Grains and their porducts* A. A. C. C.
7. Staudt, E., 1955, Proceedings of the 3rd International Bread Congress, Hamburg.
8. Greer, E. N. and Stewart, B. A., 1957, *Die Mühle*, **94,** 494.
9. Zeleny, L. and Coleman , D. N., 1938, Acidity in Cereals and Cereal Products, *Cereal Chem.*, **15,** 580.
10. Christensen, C. M., 1946, The quantitative determination of molds in flour, *Cereal Chem.*, **23,** 322.
11. American Association of Cereal Chemists, 1947, Cereal Laboratory Methods 5th, ed.
12. Kent-Jones, D. W. and Martin, W., 1950, A photoelectric method of determining the colour of flours as affected by grade, by measurements of reflecting power, *Analyst*, **75,** 127.
13. Anker, C. A. and Geddes, W. F., 1944, *Cereal Chem.*, **21,** 335.
14. Christensen, C. M. and Gordon, D. R., 1951, *Cereal Chem.*, **28,** 408.

CORRIGENDUM

Volume 7 Number 2, Page 71, please *delete* the following caption from the diagram:

Sea salt, NaCl and CaCl,

• Volume 7C, Number 4, December 1959

מוסד ויצמן לפרסומים במדעי הטבע ובטכנולוגיה בישראל • ירושלים
The Weizmann Science Press of Israel • Jerusalem

BULLETIN OF THE RESEARCH COUNCIL OF ISRAEL

Section C TECHNOLOGY

Bull. Res. Counc. of Israel. C. Techn.

Incorporating the Scientific Publications of the Technion — Israel Institute of Technology, Haifa

INDEX TO VOLUME 7C

INDEX

TO VOLUME 7C

CONTENTS

Number 4, January 1960

AUTHOR INDEX

SUBJECT INDEX

יוצא לאור ע"י

מוסד ויצמן לפרסומים במדעי הטבע ובטכנולוגיה בישראל

המועצה המדעית לישראל - משרד החנוך והתרבות - האוניברסיטה העברית בירושלים
הטכניון — מכון טכנולוגי לישראל - מכון ויצמן למדע - מוסד ביאליק

Published by

THE WEIZMANN SCIENCE PRESS OF ISRAEL

Research Council of Israel, Ministry of Education and Culture
The Hebrew University of Jerusalem, Technion–Israel Institute of Technology
The Weizmann Institute of Science, Bialik Institute

Printed in Israel

JERUSALEM ACADEMIC PRESS LTD.

SET ON MONOTYPE

WSP/1000/2.60/18